Chemical Papers (2019) 73:1547–1560
https://doi.org/10.1007/s11696-019-00710-3

ORIGINAL PAPER

Effective catalysts derived from waste ostrich eggshells for glycolysis of post-consumer PET bottles

Isti Yunita[1,2] · Siraphat Putisompon[1] · Peerapong Chumkaeo[1] · Thinnaphat Poonsawat[1] · Ekasith Somsook[1]

Received: 21 October 2018 / Accepted: 5 February 2019 / Published online: 20 February 2019

Abstract

Herein, we report an effective chemical recycling of poly(ethylene terephthalate) (PET) using sustainable sources of catalysts, calcium oxide (CaO) derived from ostrich eggshells. The active catalysts were demonstrated in the chemical depolymerization of post-consumer PET bottles. Beverage bottles were proceeded with 1 wt% catalyst derived from ostrich eggshells in the presence of ethylene glycol at 192 °C under atmospheric pressure to give the major product as bis(2-hydroxyethyl terephthalate) (BHET) which was confirmed by melting point, IR spectroscopy, ^{1}H-, ^{13}C-NMR spectroscopy and mass spectrum. The catalyst could fully depolymerize PET within 2 h, producing a good yield of highly pure BHET monomer. The catalysts were successfully characterized by X-ray powder diffraction (XRD), X-ray photoelectron spectroscopy (XPS), field-emission scanning electron microscopy with energy dispersive X-ray spectroscopy analysis (FE-SEM), and thermogravimetric analysis (TGA). Furthermore, catalysts derived from chicken eggshells, geloina, mussel, and oyster shells were run to compare the catalytic activities. For better understanding of catalytic parameters, effects of calcination temperatures of catalyst, weight ratio of catalyst, ratio of weight of solvent, and time of depolymerization for the ostrich eggshells catalyst were also investigated.

Keywords Ostrich · Eggshells · Glycolysis · Poly(ethylene terephthalate) · Depolymerization

Introduction

Drinking bottles are plastics made from poly(ethylene terephthalate) (PET) with the highest consumption growth. The demand for poly(ethylene terephthalate) bottles is progressing with dramatic applications in beverage containers (López-Fonseca et al. 2011). PET resins are also in demand for flexible packaging films due to its high clarity, low permeability, and excellent printing capabilities. However, PET waste poses an indirect hazard to the environment. It has high resistance to atmospheric and biological substances. This material is considered as a harmful substance that causes chain of environmental damages (Webb et al. 2013). Thus, this phenomenon, an issue related to human viability, is the main reason for PET waste recycling to gain more attentions today (Khoonkari et al. 2015).

Four major approaches have been proposed for PET recycling: "in-plant" recycling, mechanical recycling, chemical recycling and energy recovery through incineration (López-Fonseca et al. 2010). However, some researchers have endeavored to develop methods that essentially involve the recovery of monomers and the production of chemicals with attractive added value or intermediates of PET wastes. Among those methods, chemical recycling materials show the highest consistency with the principle of sustainable development leading to the recovery of raw materials from PET which have been made (Imran et al. 2013).

There are several chemical recycling methods proposed for PET depolymerization, such as hydrolysis, methanolysis, ammonolysis, aminolysis, and glycolysis. The glycolysis is the most effective method for the production of a high-priced virgin monomer, bis(2-hydroxyethyl terephthalate) (BHET) by breaking down the ester bond followed by the

✉ Ekasith Somsook
ekasith.som@mahidol.ac.th

[1] NANOCAST Laboratory, Center for Catalysis Science and Technology, Department of Chemistry and Center of Excellence for Innovation in Chemistry, Faculty of Science, Mahidol University, 272 Rama VI Rd., Thung Phaya Thai, Ratchathewi, Bangkok 10400, Thailand

[2] Department of Chemistry Education, Yogyakarta State University, Colombo Road No. 1, Yogyakarta 55281, Indonesia

replacement of the hydroxyl terminal (George and Kurian 2014). This product can be easily integrated into a conventional PET manufacturing plant. Furthermore, this monomer can be used as a building block for other polymer syntheses with higher economic value, ranging from unsaturated polyester resins and polyethylene terephthalate (PET) to a new biocompatible system (Wang et al. 2009). From these points of views, it can be concluded that this process is promising for environmental sustainability.

Catalysts play a key role in the glycolysis to obtain a maximum yield (Nica et al. 2015). One of the various catalysts commonly used in PET glycolysis is zinc acetate, as the activation of reaction by this catalyst is remarkable (Xi et al. 2005). Other salts, such as metal acetate (Co, Pb, and Mn) (Ghaemy and Mossaddegh 2005), chloride (Zn, Li, Didymium, Mg, and Fe) (Pingale et al. 2010), titanium phosphate (Troev et al. 2003), hydroxide (Li, K) (Shukla and Harad 2005; Nikje and Nazari 2007), sulphate (Na, K) (Shukla and Harad 2005), and sodium carbonate (Duque-Ingunza et al. 2013; Shukla and Kulkarni 2002) have been investigated. Recently, a series of novel catalysts in the process of glycolysis, including Lewis acid ionic liquids (Al-Sabagh et al. 2014; López-Fonseca et al. 2010; Wang et al. 2009) and metal oxides (Imran et al. 2011, 2013), have been studied. In addition, different methods for using microwave irradiation on PET glycolysis have also been reported (Choudhary et al. 2013; Pingale and Shukla 2008), but it has a shortcoming like the use of a sophisticated set of instruments. However, these ionic liquids catalyst is impractical in synthetic process, has high toxicity and erosivity, lower percentage in PET conversion and BHET selectivity compared to metal oxide as a catalyst (Al-Sabagh et al. 2014; Imran et al. 2011, 2013; López-Fonseca et al. 2010; Wang et al. 2009). Many efforts have been made by researchers to find affordable catalysts and reaction systems.

Various heterogeneous catalysts based on metal oxides have been tested in PET glycolysis. Imran et al. (2013) reported that mixed-oxide spinels showed high catalytic activity when tested on PET glycolysis at 260 °C with a pressure under 5.0 atm. Park et al. (2012) investigated glycolysis of post-consumed PET using graphene oxide–manganese nanocomposite (GO–Mn_3O_4) in a stainless-steel batch autoclave reactor at 300 °C and 1.1 MPa for 80 min. The lowest amount of Mn_3O_4 loading on graphene oxide (GO) yields the highest percentage of BHET about 96.4%, whereas in PET glycolysis with Mn_3O_4 without graphene oxide (GO) produced 82.7% yield of BHET. Bartolome et al. (2014) reported the high yields of BHET after 1 h of glycolysis at 300 °C using γ-Fe_2O_3 nanoparticles.

The utilization of high temperature, sophisticated apparatus and high pressure is seen as major disadvantages for the use of these catalysts in PET glycolysis. Al-Sabagh et al. (2016) reported that Fe_3O_4-boosted multiwalled carbon nanotubes (MWCNT) as a sustainable and friendly catalyst in PET glycolysis with 100% yield of BHET at 190 °C for 2 h. Using metal oxide as a catalyst in the glycolysis can be a promising alternative process in addition to using conventional catalysts. It is associated with high monomer yield, high mechanical strength, high reusability, and ease of separation. More over, low temperatures succesfully applied in those work (Al-Sabagh et al. 2016), although, the high quality of catalyst was difficult to be denied as it was an important factor to enhance the percentage of yield.

The aims of this investigation are to prepare Ca-based metal oxide derived from by-products of food sources and then to apply them as catalysts in the glycolysis of waste drinking bottles made from PET to solve waste problems. The sources of calcium to be used are household wastes from eggshells and seafood shells. To the best of our knowledge, there is no report on the production of calcium oxide from ostrich eggshells, chicken eggshells or various shells as catalysts for the glycolysis of poly(ethylene terephthalate).

In this study, calcium oxide catalysts made from various calcium sources were prepared, characterized and tested in the glycolysis of waste drinking bottles made from PET.

Experimental

Materials

Post-consumer PET bottles were collected, further cleaned, and cut into 3×3 mm^2 square chips after lids, label and bottom parts were removed. Flake PET was cleaned by 1 mol dm^{-3} of sodium hydroxide solution, type 1 ultrapure water and dried at 80 °C for 12 h. Ethylene glycol (EG) (analytical grade) was purchased from RCI Labscan. Ostrich eggshells, chicken eggshells, oyster shells, geloina shells, and mussel shells were collected from local markets.

Preparation of catalysts

All shells were cleaned and dried before crushing and sifting to yield powder. The dried waste shells are calcined at a temperature of 600–1000 °C in the air atmosphere with a heating rate of 5 °C min^{-1} for 5 h. All calcined samples are stored in a desiccator to avoid moisture in the air before use.

Glycolysis of PET

Each experiment was repeated for 3 times. The glycolysis reaction was set in a 100 cm^3 two-neck round bottle equipped with a magnetic stirrer with condenser and thermometer. 5 g of flake PET, desired catalyst (the weight ratio of catalyst to EG of 0.01, 0.02, 0.05, 0.1), and ethylene glycol (the weight ratio of EG to PET of 5, 10, 15, 20) were mixed and the

reaction temperature was set at 192 °C with varying reaction times (in the range 1 until 4 h). After completion of glycolysis, the obtained product was frozen for 12 h followed by extraction with 500 cm^3 of boiling distilled water. The mixture was separated into solid and liquid phases by filtration. The solids were washed, dried, and weighed as oligomers. All filtrates were heated at 90 °C until a clear extract solution existed. Flake BHET obtained from the liquid phase with vacuum filtration after being stored in freezer at 0 °C for 12 h was transferred to a chiller for 24 h.

The obtained BHET flakes were then washed with cold water and dried at 80 °C for 12 h and the weight of the BHET result was used for the calculation of yield of BHET. The conversion of PET is defined by Eq. (1) and yield of BHET product was calculated by Eq. (2).

$$\text{Conversion of PET} = \frac{u_1}{u_0} \times 100\% \quad (1)$$

$$\text{Yield of BHET} = \frac{\left(m_1/\text{MW}_{\text{BHET}}\right)}{\left(m_0/\text{MW}_{\text{PET}}\right)} \times 100\% \quad (2)$$

In the equation, u_0, u_1 represented initial weight and undepolymerized weight of PET. m_0, m_1 represented theoretical weight and actual weight of BHET. MW_{BHET} and MW_{PET} refer to the molecular mass of BHET which is 254 g mol^{-1} and PET repeating unit which is 192 g mol^{-1}, respectively.

Characterization

The morphology, structure and elemental analyses of calcium oxide from waste shells-derived catalyst were utilized by field-emission scanning electron microscopy (FE-SEM, Hitachi SU8010) which has SE resolution 1.3 nm and field emission tip as the filament source. The micrographs were taken in various magnifications at electron acceleration voltage of 4.0 kV. Using the same instrument, the analysis by energy dispersive X-ray spectroscopy (EDX) was conducted at electron acceleration voltage of 15 kV.

X-ray photoelectron spectroscopy (XPS) was obtained from Axis Ultra DLD, Kratos Analytical Ltd., UK. X-ray powder diffraction (XRD) characterization of the waste-shells catalyst was completed using Bruker D8 Advance diffractometer (Germany) with Cu-Kα radiation ($\lambda = 0.15418$ nm), 30 kV and 15 mA over a 2θ range of 10° to 80° with a step size of 0.02° at a scanning speed of 6°/min.

Thermo-gravimetric analysis–differential scanning calorimetry (TGA–DSC) was performed using a TA instruments SDT2960 simultaneous at the heating rate of 20 °C min^{-1} in the range from room temperature to 900 °C under nitrogen gas.

^{1}H- and ^{13}C-NMR spectra of the isolated product in DMSO-d_6 were collected on a 400-MHz Bruker Avance NMR Spectrometer. The NMR parameters were set up at 16 and 512 scans, relaxation times of 1 s and 1.5 s, pulse widths of 15 and 11 μs for ^{1}H- and ^{13}C-NMR spectra, respectively. Gas chromatography with mass spectrometry (GCMS) spectra were obtained by Agilent 7950 (GC) and Agilent 5975 (MS) with an HP-5 capillary column. Electrospray ionization (ESI, *m/z*) mass spectrometry was performed using microTOF in positive ion mode. Fourier transform-infrared spectroscopy (FT-IR) analysis was performed using Perkin Elmer Series Spectrometer (Frontier Model), in the range of 4000–400 cm^{-1}.

Results and discussion

Morphology, structure and elemental analyses of catalysts

The XRD patterns of calcined shells are shown in Fig. 1. All samples were calcined at 1000 °C for 5 h. After calcination, it was observed for the transformation of $CaCO_3$ to CaO for seafood shells and eggshells. The main diffraction peak was in good agreement with the JCPDS card no. 00-002-1088 from typical cubic CaO crystals. Therefore, the occurrence of intense and narrow peaks in calcined solids defines the crystal structure of calcium oxide as a compound, indicating that the catalyst must be activated thermally before being used in the reaction of glycolysis. In addition, traces of $Ca(OH)_2$ impurities derived from the reaction of CaO and water in the air were found at 2θ of 18.3° in a good agreement with the JCPDS card no. 87-0674.

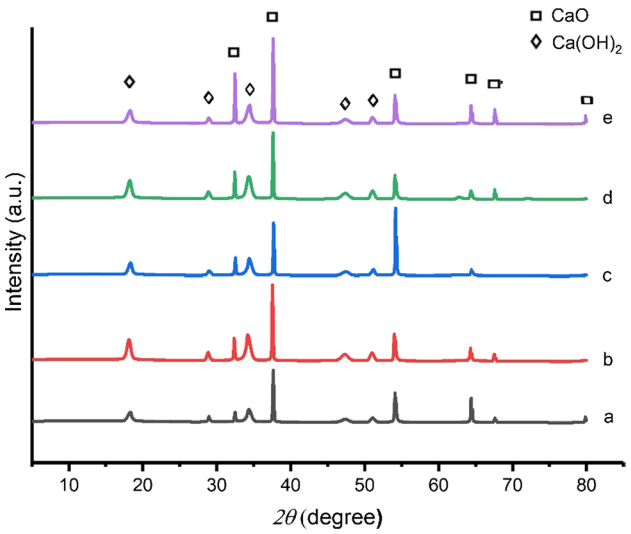

Fig. 1 XRD patterns of **a** geloina, **b** chicken, **c** mussel, **d** oyster, **e** ostrich eggshells

Due to the excellent mechanical properties of ostrich eggshells, they were selected for the further studies in the calcination of samples at different temperatures for 5 h as shown in Fig. 2. In the diffractograms of uncalcined ostrich eggshells and calcined ostrich eggshells at 600 °C and 700 °C, the peaks associated with $CaCO_3$ at $2\theta = 23°$, 30°, 37°, 44°, 48°, 49°, 58°, 61°, and 65.2° (in the agreement with JCPDS file no. 47-1743) were observed. As the temperature for the calcination increased, it resulted in the change in the composition of the ostrich eggshells. The peaks for calcined ostrich eggshells at 1000 °C for 5 h showed identical, clear and sharp reflection peaks at 2θ of 35°, 38°, 54°, 64° and 68°, the characteristic peaks of calcium oxide (JCPDS file no. 00-002-1088), which indicates a single crystalline phase.

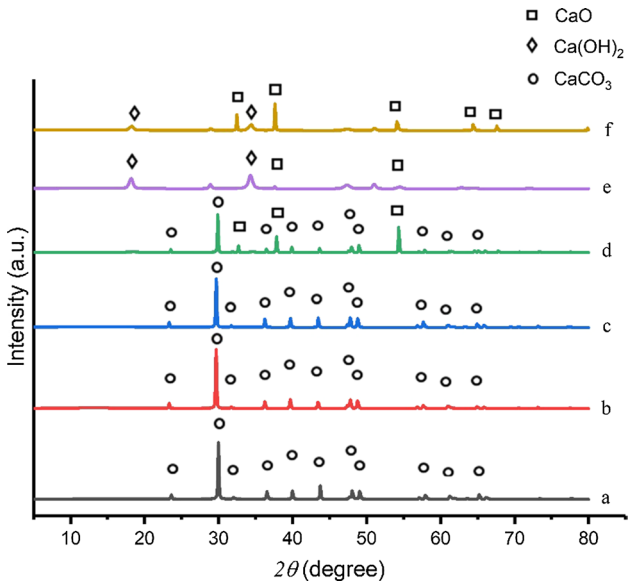

Fig. 2 XRD patterns of **a** uncalcined ostrich eggshells, calcined ostrich eggshells at **b** 600 °C, **c** 700 °C, **d** 800 °C, **e** 900 °C, **f** 1000 °C

The CaO lattice constant of the sample is determined by identifying the peak position (2θ) of the XRD pattern using Bragg's Law. The lattice constants in the sample were found to be 4.7418 Å, which corresponded to the lattice constant in pure CaO.

The morphology and elemental analyses of shells were examined by FE-SEM/EDX at 4.0 kV and 15 kV of the acceleration voltage, respectively, after coating with Pd/Pt, due to the non-conductivity of calcium oxides as shown in Figs. 3 and 4. Calcined chicken, geloina, mussel and oyster shells in Fig. 3 show the morphological similarities of particles with calcined ostrich eggshells. The calcined waste shells showed a regular shape and most of them were bound together as aggregates with varying aggregate sizes. However, larger sizes of aggregates were observed on ostrich eggshells, which were detected as groups of agglomerated particles from small particles, ranging up to several tens of microns (Viriya-empikul et al. 2012). In this case, the smaller grain size and aggregate provided a higher specific surface area. On the other hand, the higher magnification showed the layered surfaces which were the same characteristic of cracking on the all types of shells.

The presence of irregular particle shapes from ostrich eggshells at Fig. 4 before calcination was significant. The size of the calcined ostrich eggshells particles decreased and the shape of the particles became more regular along with the calcination process. The microstructural architectures of shells were not changed drastically from layered to porous structures (Buasri et al. 2013).

The small particles in the calcined ostrich eggshells combined to make large agglomerates that could be observed after calcination at a temperature of 800 °C and continue to enlarge after calcination at a temperature of 1000 °C. The agglomeration of the calcined catalyst was caused by the formation of sufficiently uniform oxides. Changes in the shells structure could be caused by changes in composition. Calcium carbonate which was a largest part of the components

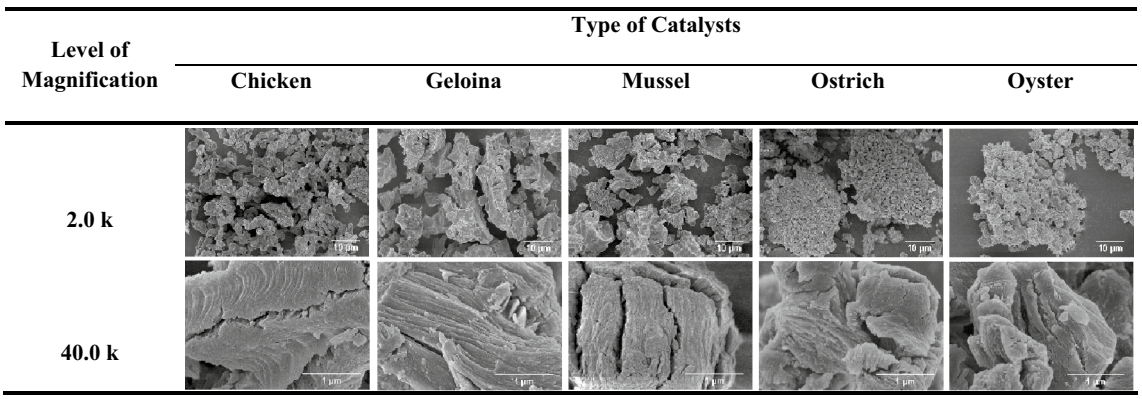

Fig. 3 FE-SEM images of calcium oxide particles obtained from calcined different shells

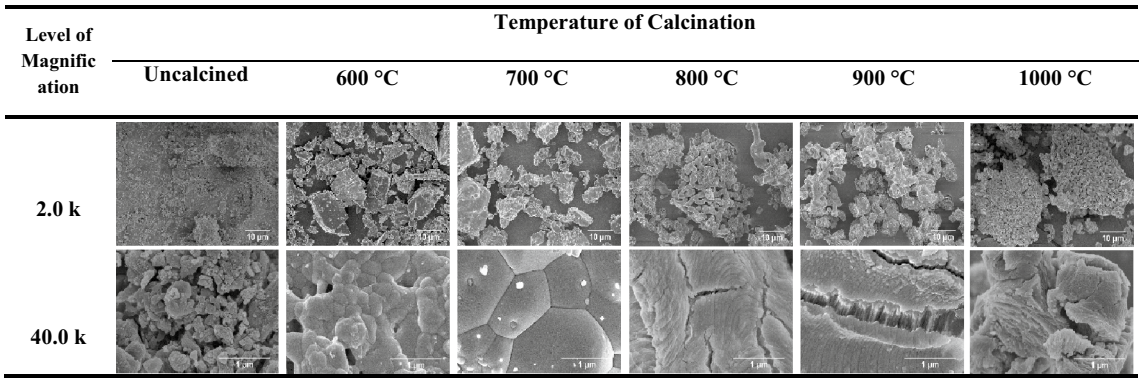

Fig. 4 FE-SEM images of ostrich eggshells obtained from different temperatures of calcination

Table 1 Elemental analysis of the calcined catalysts at 1000 °C, uncalcined ostrich eggshells and their atomic/weight concentrations (%) determined by FE-SEM–EDX

Catalyst	Weight % of element		Atomic % of element	
	Ca K	O (K)	Ca K	O (K)
Chicken	60.55	39.45	37.99	62.01
Geloina	54.46	45.54	32.32	67.68
Mussel	54.41	45.59	32.27	67.73
Oyster	49.96	50.04	28.50	71.50
Ostrich	65.26	34.74	42.85	57.15
Uncalcined ostrich	47.00	53.00	26.15	73.85

contained in the shell broken down into CaO by evolving carbon dioxide upon the heating process.

The ostrich eggshells that were calcined at 600 °C and 700 °C exhibited irregular and modulated non-uniform particle shapes. Furthermore, ostrich eggshells which were calcined at higher temperatures, after 800 °C, showed microstructures of calcium oxide. After applying the high temperature of calcination, the morphology of the catalyst was changed from irregular shapes to interconnected forms such as skeletal structures. Some surface cracks in SEM images were observed from the changing of the calcination temperature in SEM images. In addition, calcium oxide as a necessary active site in the reaction of glycolysis is successfully produced, which is supported by XRD diffractogram.

Analysis of the elemental composition of samples is shown in Table 1. The elements determined were Ca and O. Calcined ostrich eggshells had the highest calcium and oxygen deposits on the outer surface, each of which was 65.26% and 34.74% by weight of the element. The amounts of calcium in calcined oysters and uncalcined ostrich eggshells were slightly different.

As shown in Fig. 5, the thermograms of uncalcined samples show two different stages of weight loss: one at a temperature below 700 °C and the other stage occurring between 700 and 800 °C. The waste eggshells were analyzed by TGA/DSC to determine the appropriate calcination temperature to produce calcium oxide as the catalyst for glycolysis. The thermal behaviors of different type uncalcined catalysts showed the similar pattern of TGA curve, which had a different stage of weight loss. At a temperature below 370 °C, it was associated with evaporation of moisture which was physically trapped in the eggshells and also removing the organic matter; furthermore, the weight loss continued after 370 °C–550 °C associated with dehydration of $Ca(OH)_2$ (~4 wt%). The next decomposition was occurred from 700 °C and end around 800 °C, found throughout 5 samples, which showed the dissociation of remaining organic material and the presence of calcium carbonate. The major weight loss around those temperatures, ~42 wt%, was due to the transformation of $CaCO_3$ phase to CaO phase and carbon dioxide as the by-product. As the sample weight remained constant after 800 °C and the main composition of the sample calcined at and above 900 °C is calcium oxide, confirmed by XRD diffraction, the temperature of 1000 °C was suitable for the use as the calcination temperature to ensure complete conversion into CaO, confirmed by the TGA and DSC curves (Viriya-empikul et al. 2012). The results of the TGA analysis were supported by the results of the DSC analysis. The endothermic peak that occurred at 760 °C proved the decomposition of $CaCO_3$ to CaO.

A slightly different finding in the TGA curve in each shell was in agreement with Mohamad et al. (2016) that smaller particles undergo rapid changes compared to larger particles. This observation may be due to the large surface area associated with smaller particle size that contributes to higher heat exchange rates needed to promote decomposition (Mohamed et al. 2012).

X-ray photoelectron spectroscopy (XPS) is the important technique for the elucidation of the catalyst surface composition and the chemical state of its constituent elements. Table 2 shows the binding energy (BE) values (in eV) and

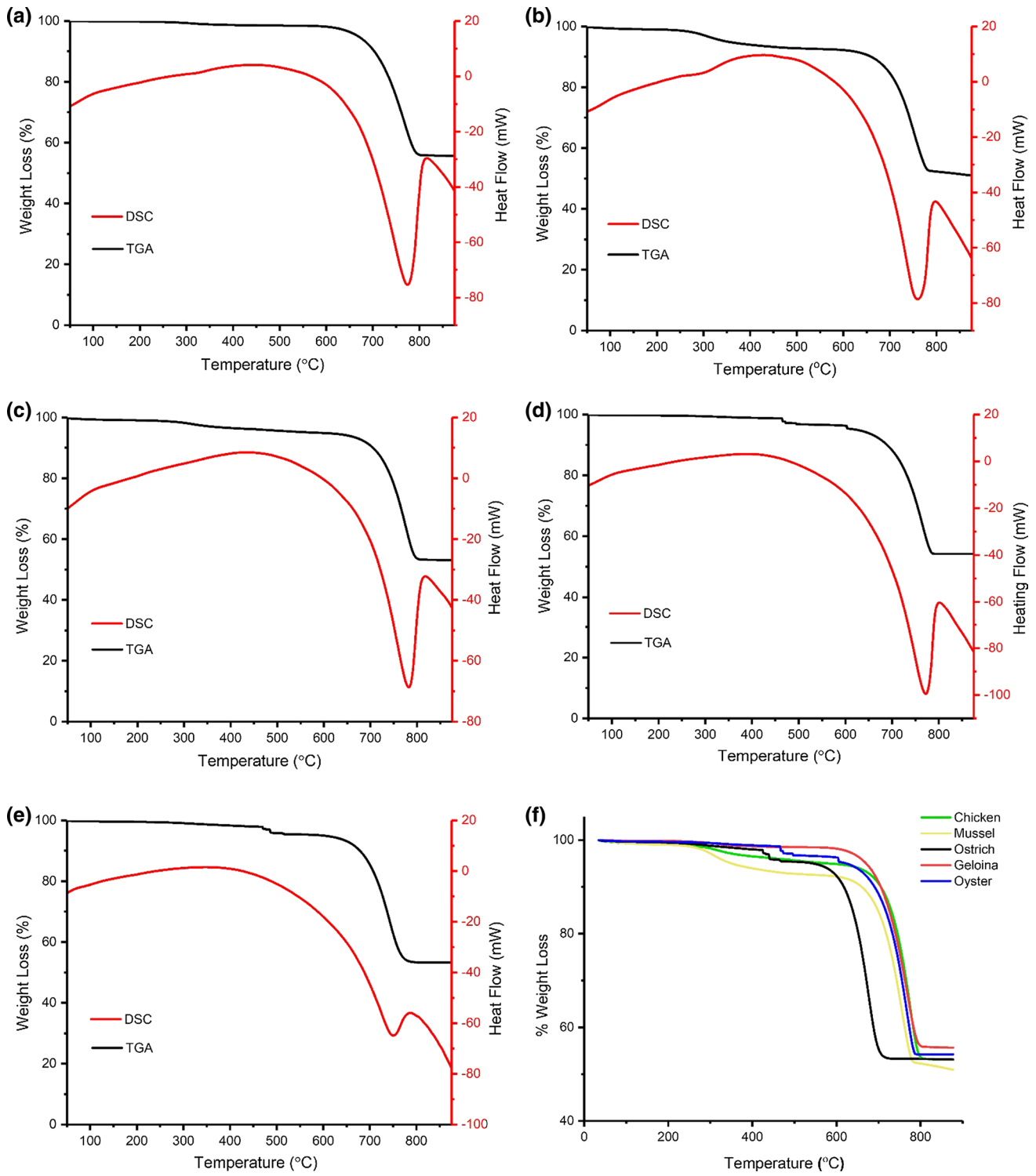

Fig. 5 TGA curves of **a** geloina, **b** mussel, **c** chicken, **d** oyster, **e** ostrich, **f** all shells

atomic concentration values (in %) of elements from ostrich and calcined ostrich eggshells.

The XPS data revealed that the uncalcined and calcined ostrich eggshells predominantly confined oxygen, calcium and carbon element. In the uncalcined ostrich eggshells (Fig. 6), the relative mass ratio for oxygen, calcium and carbon is 37.82%, 29.14% and 33.03%, respectively. On the contrary (Fig. 7), after calcination at 1000 °C, the resultant

Table 2 Binding energy values of the constituent elements of uncalcined and calcined eggshells and their atomic concentrations (%) determined by XPS

Element	Uncalcined ostrich eggshell		Calcined ostrich eggshell at 1000 °C	
	BE (eV)	% atomic concentration	BE (eV)	% atomic concentration
O 1s	531.2	40.47	530.8	32.1
	–		531.8	15.7
	–		533.4	1.5
Total O				49.3
Ca 2p	–	–	346.3	6.1
Ca 2p	347.0	8.45	347.2	7.4
Ca 2p	–	–	349.7	3.1
Ca 2p	350.6	4	350.6	3.4
Total Ca		12.45		20

displayed mainly three typical peaks of O 1s, Ca 2p, and C 1s in relative mass ratios between oxygen and calcium for 1:1, vis. 40.34%, 40.84%, and 18.82%, respectively. The Ca 2p spectrum on the calcined ostrich eggshells, showed four relative calcium species, which corresponded to Ca^{2+} in CaO, in the form of Ca $2p^{3/2}$ (346.3 eV) and (347.2 eV), Ca $2p^{1/2}$ (349.7 eV) and (350.6 eV). The C 1s spectrum could be deconvoluted into three peaks corresponding to the presence of carbon and organic matter (284.5 eV), C–O (285.8 eV), and O–C–O and C=O (289.4 eV) functional groups. In addition, the deconvolution of the O 1s spectrum at calcined ostrich eggshells revealed peaks originating from O^{2-} (530.8 eV) were determined to be metal oxide, adsorbed water (H_2O at 533.4 eV), predominant existence of OH^- groups (531.8 eV).

Effect of different catalysts on the depolymerization of drinking water bottles

The formation of calcium oxide in each shell after calcination at the temperature of 1000 °C was the main reason for using calcined eggshells at 1000 °C to study the effects of various shells in the reaction of glycolysis. Glycolysis reaction with commercial zinc acetate ($Zn(OAc)_2$) as the catalyst was set as a controlled experiment. Zinc salt is a well-known catalyst used in glycolysis with high-yield products. From this work, 75% yield of BHET was obtained using 1 wt% of commercial $Zn(OAc)_2$. This result was slightly different with the reaction using calcined ostrich eggshells which can produce 76% yield of BHET (Fig. 8). Catalysts derived from ostrich eggshells showed the best catalytic activity which produced the highest yield percentage and were selected for the further studies. According to the result in Fig. 8, the higher calcium content in the catalyst did not guarantee the

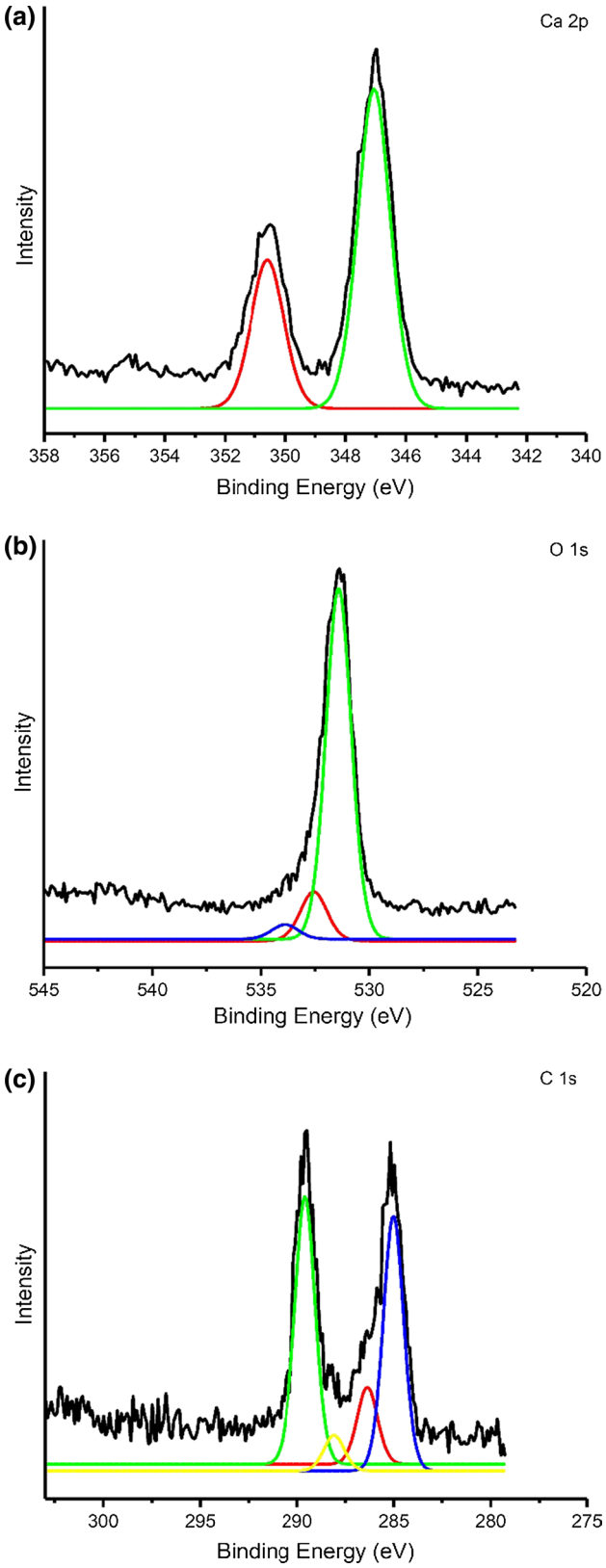

Fig. 6 XPS spectra of uncalcined ostrich eggshells showing the fitted peaks **a** Ca 2p, **b** O 1s, **c** C 1s

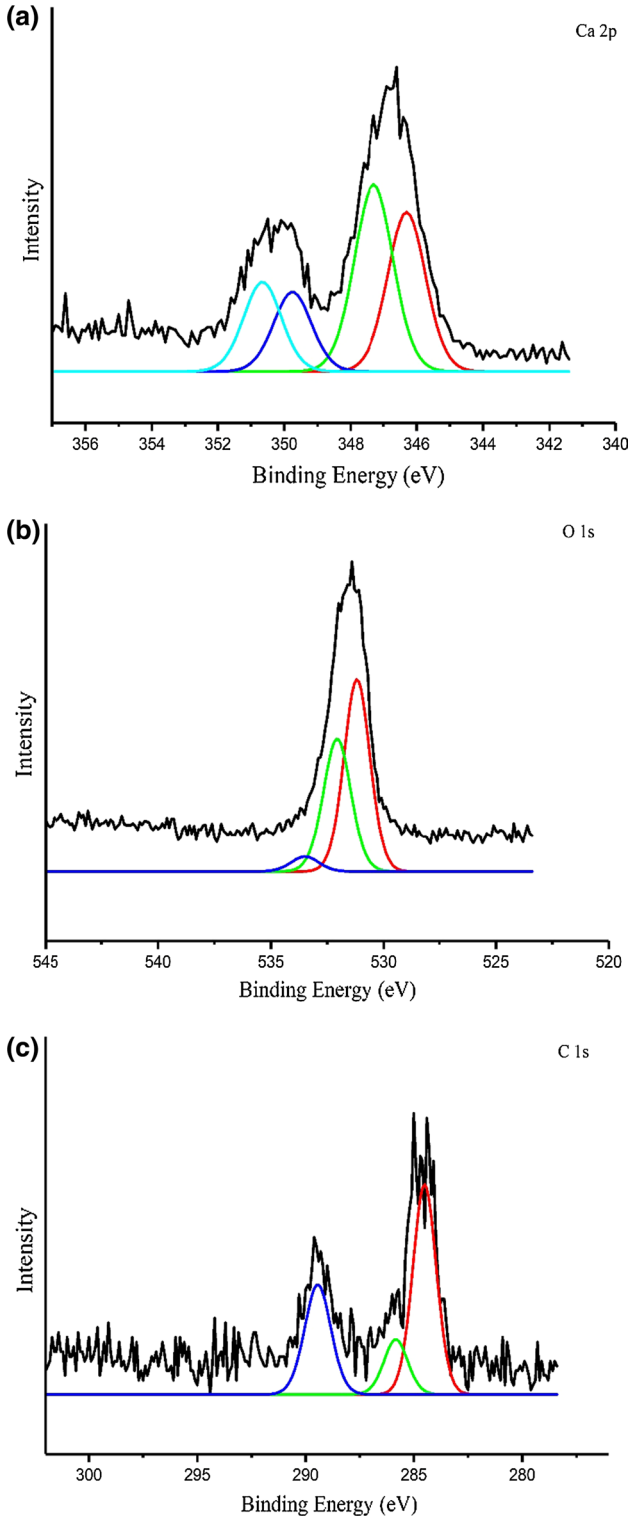

Fig. 7 XPS spectra of calcined ostrich eggshells at 1000 °C showing the fitted peaks **a** Ca 2p, **b** O 1s, and **c** C 1s

higher yield of BHET products. This fact was consistent with data obtained in glycolysis reactions using catalysts derived from mussel and geloina shells which produced 63% and 61% yield of BHET, respectively. Both of these catalysts contained around 54% by weight of calcium.

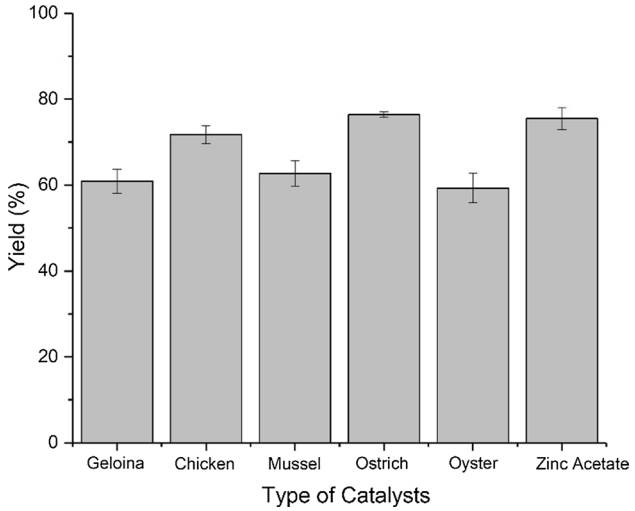

Fig. 8 The effect of different catalysts on the yield of BHET. Reaction was set at 192 °C for 2 h. All types of catalyst were loaded at 1 wt% into each batch and the ratio between PET and ethylene glycol was 1:15. 100% conversion

Effect of calcination temperatures of catalysts

The effect of calcination temperature of catalysts derived from ostrich eggshells on the glycolysis was investigated as shown in Fig. 9. It was clear that increase in temperature for calcination of catalyst increased the catalytic activities. According to XRD data, the peak of CaO became clearer and was formed by increasing the temperature of calcination. No significant fouling or second phase was detected, which showed that high purity of CaO was obtained. The crystallinity of CaO increased linearly during the sintering process until the calcination temperature reaches 1000 °C. This was the reason that catalyst derived from ostrich eggshells calcined at 1000 °C was proved to be the most effective catalyst. Hereafter, in the case of ostrich eggshells, based on the TGA/DSC analysis, it was shown that the conversion of $CaCO_3$ into CaO occurred exquisitely at temperatures above 900 °C which were followed by completely releasing of CO_2 (Tan et al. 2015).

Effect of weight ratio of PET–ethylene glycol

In our study, the effect of weight ratio of PET–ethylene glycol (EG) on the resulting product yield was also investigated as shown in Fig. 10. It can be seen that the observed catalyst performance increased when the weight ratio of PET to ethylene glycol applied in glycolysis system with catalyst derived from ostrich eggshells calcined at 1000 °C was 1:15. On the other hand, when the weight ratio of PET–ethylene

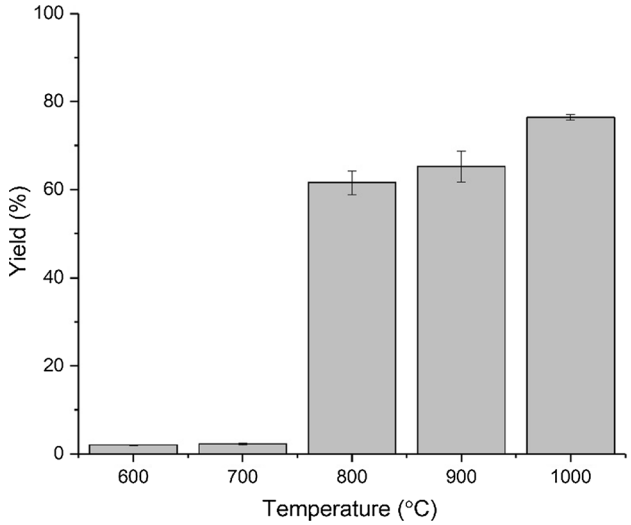

Fig. 9 The effect of calcination temperatures on the catalytic activity of ostrich eggshells for glycolysis of water bottles. Reaction was set at 192 °C for 2 h. All types of catalyst were loaded at 1 wt% into each batch and the ratio between PET and ethylene glycol was 1:15. 5% of conversion on the 600 °C and 7% of conversion on the 700 °C

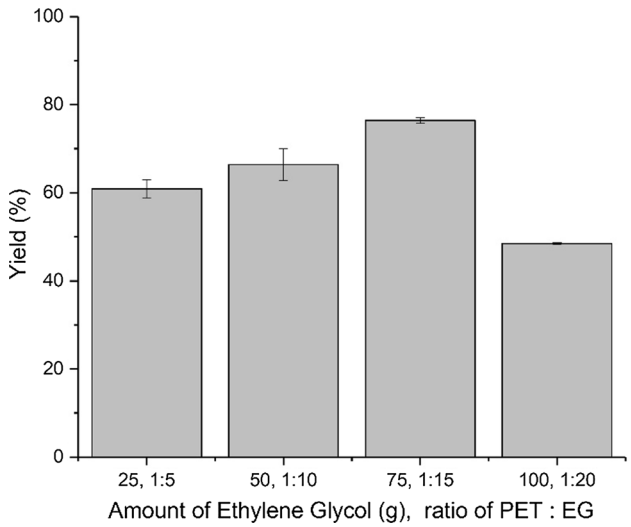

Fig. 10 The effect of weight ratio of PET–EG on the yield of BHET. Reaction was set at 192 °C for 2 h, 5 g of PET. Catalyst was loaded at 1 wt% into each batch. 100% conversion

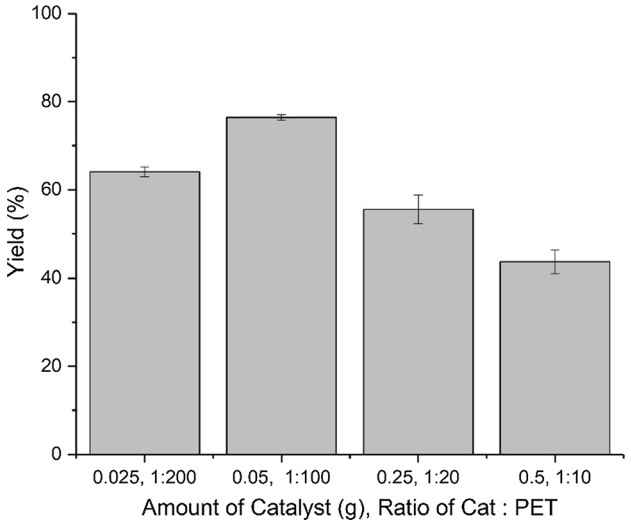

Fig. 11 The effect of weight ratio of catalyst–PET on the yield of BHET. Reaction was set at 192 °C for 2 h, 5 g of PET. The ratio between PET and ethylene glycol was 1:15. 100% conversion

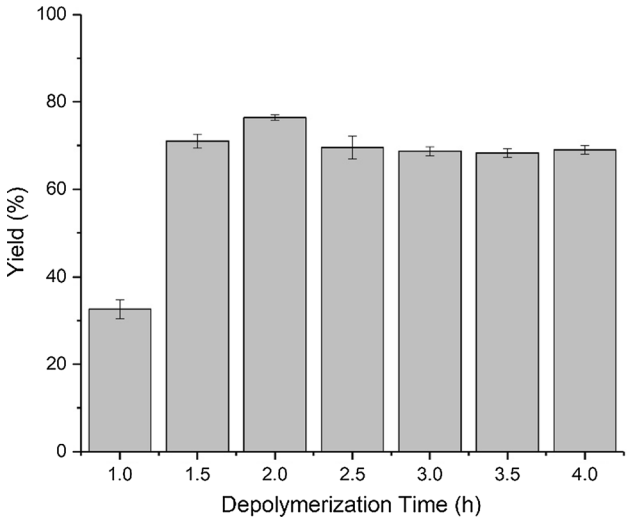

Fig. 12 The effect of depolymerization time on the yield of BHET. Reaction was set at 192 °C, 5 g of PET. Catalyst was loaded at 1 wt% into each batch. The ratio between PET and ethylene glycol was 1:15. 100% conversion

glycol was less than 1:15, the percentage of BHET was below 70%. Due to an increase in the PET–EG ratio, this will lead to an increase in the rate of decomposition and produce oligomers of lower molecular weight. However, when the ratio of PET–EG reaches the optimal value, there will be a balance between EG, oligomers, and fixed BHET, so that the degradation rate reaches a constant value. Whereas, a high proportion of PET–EG ratio, resulted in mixing difficulties in the glycolysis reactions (Jehanno et al. 2018).

Effect of weight ratio of catalyst–PET

The effects of catalyst loading were investigated and the results are demonstrated in Fig. 11. A similar catalytic performance in the 100% conversion was observed for the catalyst derived from ostrich eggshells calcined at 1000 °C. The major component of catalyst was calcium oxide. Therefore, the BHET production was investigated for the ratio of calcium oxide–PET. By increasing the catalytic loading to 5%

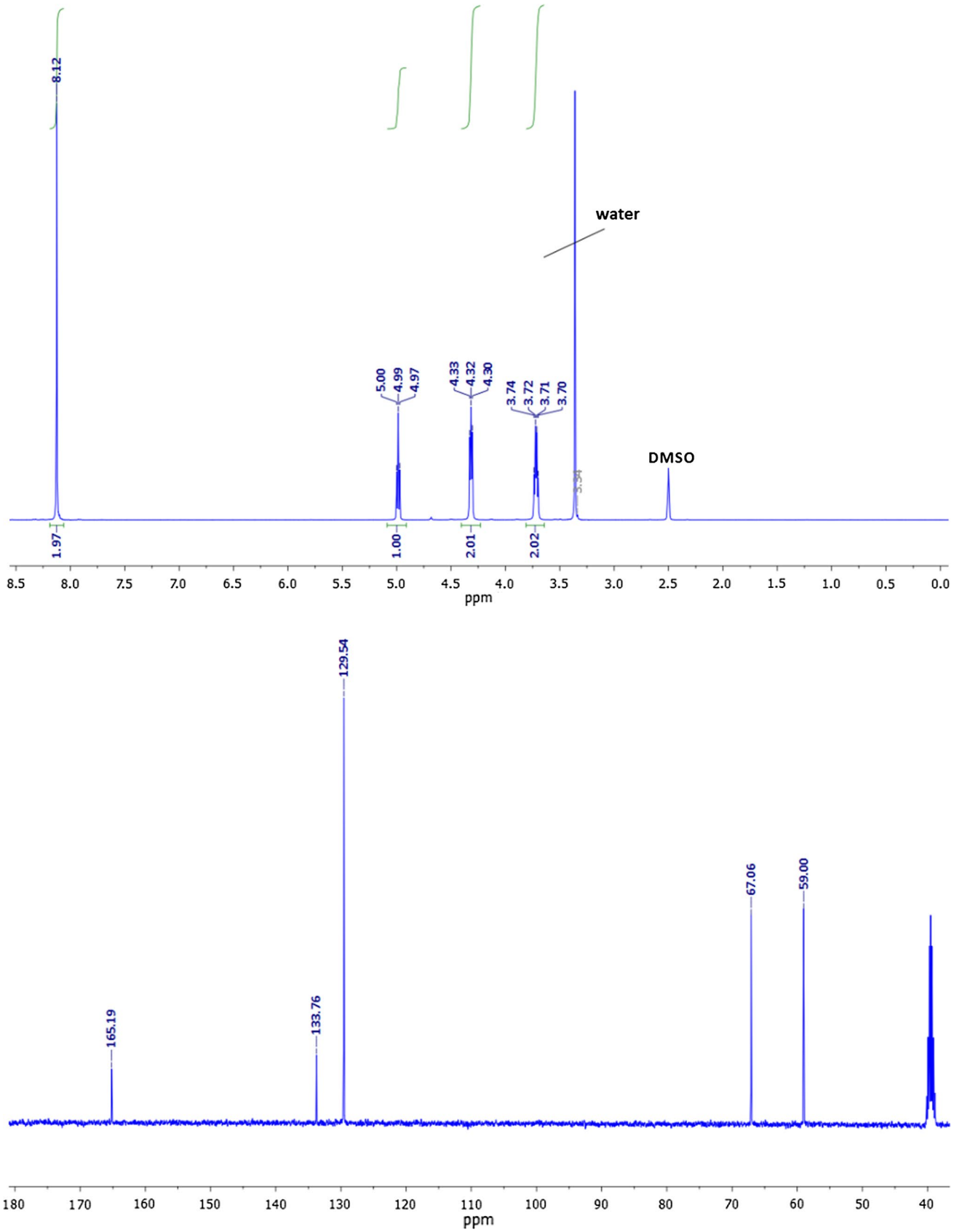

Fig. 13 ^{1}H- and ^{13}C-NMR spectra of BHET product

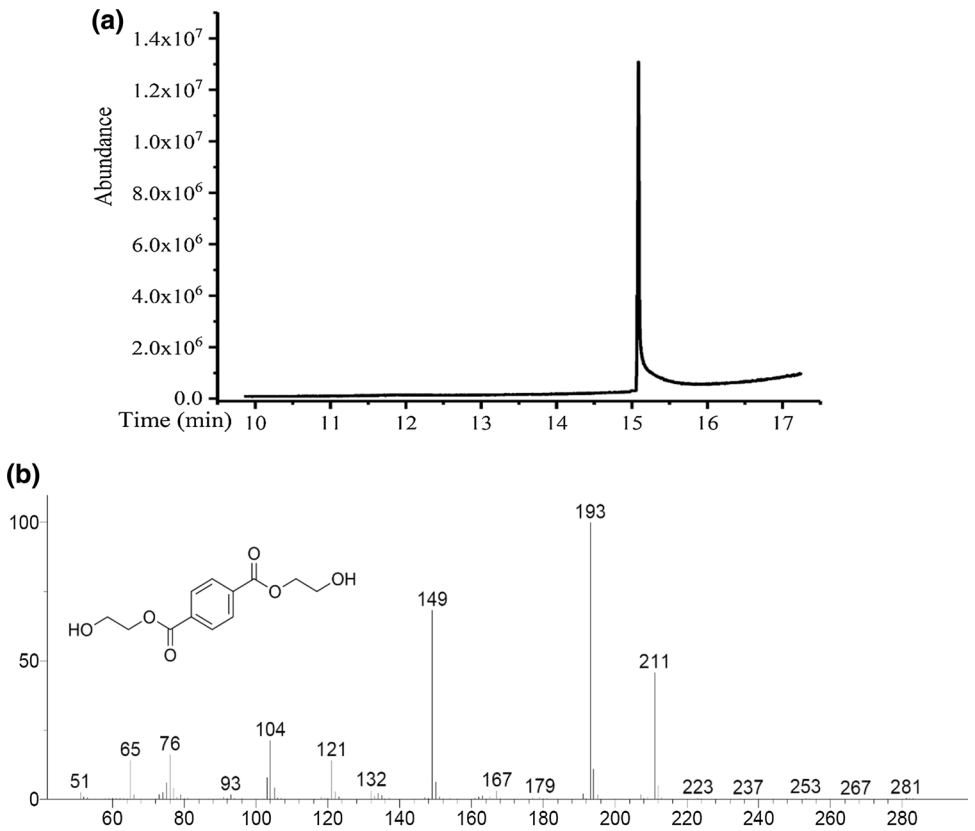

Fig. 14 **a** GC chromatogram of BHET product, **b** mass spectrum of BHET product

by weight and continued to 10% by weight, the catalytic activities of catalyst were lowered. The high possibility may be due to the high composition of calcium in the system inducing generated of by-product from the side reactions. The highest yield of glycolysis product is obtained at 1% by weight of catalyst loading, which has 100% conversion and 76% of BHET yield. This result was promising as compared to the percentage yield produced by the reaction using commercial zinc acetate as a catalyst. Likewise, reduction in yield was obtained due to reduction in catalyst loading, which resulted in 36% of oligomers and 64% of BHET, referring to Fig. 11. The reduction in BHET results was continued by increasing the catalyst concentration to 5% by weight of the substrate.

Effect of the depolymerization time

To determine the effect of depolymerization time on the yield of product, the glycolysis of PET was performed using 1 wt% of catalyst derived from ostrich eggshells calcined at

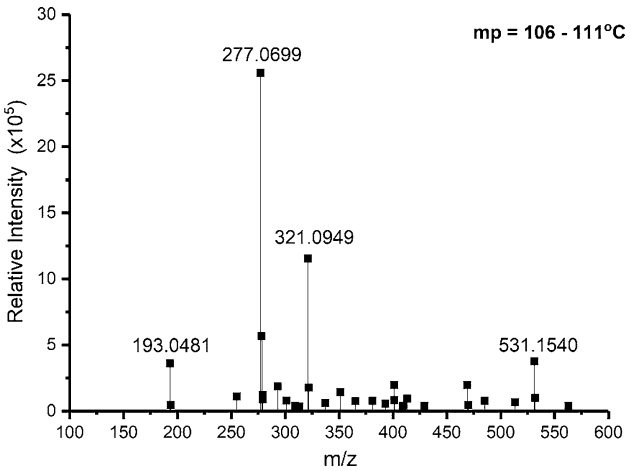

Fig. 15 ESI–MS spectrum of BHET product

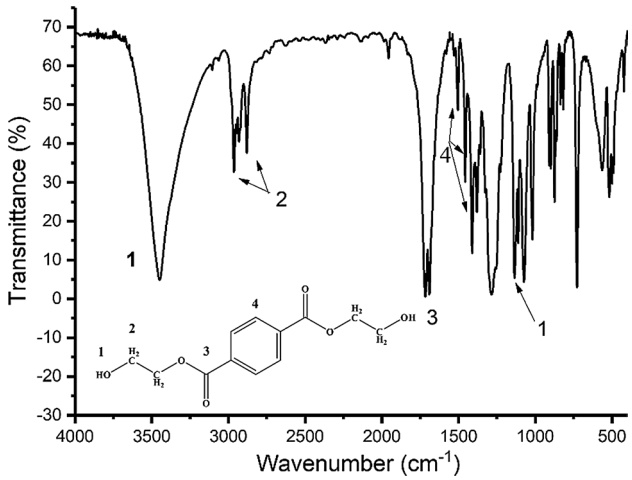

Fig. 16 FTIR spectra of BHET product

Table 3 Functional group frequencies of BHET determined by FTIR (Zhao et al. 2018)

Wave number (cm^{-1})	Types of vibration	Functional groups
3448.72	Stretching	O–H band
2963.96	Stretching	C–H alkyl
2880.14	Stretching	C–H alkyl
1716.11	Stretching	C=O group
1504.25	Stretching	C=C aromatic
1411.59	Stretching	C=C aromatic
1135.40	Stretching	C–O band

1000 °C as shown in Fig. 12. It can be seen that the BHET yield increases by lengthening the reaction time. In the presence of the catalyst, the PET conversion reached 100% within 1 h with 33% of the BHET yield. The yield of BHET increased to 71% as the reaction time was extended to 1.5 h. Furthermore, when the reaction time was extended to 2 h, the BHET yield reached the highest value of 76%. The augment of reaction time for more than 2 h does not show a significant increase in BHET.

To confirm that the major product of glycolysis was BHET, ^{1}H- and ^{13}C-NMR spectra of the BHET product were confirmed as shown in Fig. 13. The signal at δ 8.12 ppm indicated the presence of four aromatic protons from the benzene ring (δ_H = 8.12 ppm, s, 4H). Signals at δ 4.32 ppm and δ 3.71 ppm were characteristics of the methylene protons of CH_2–COO (δ_H = 4.32 ppm, t, 4H) and CH_2–OH (δ_H = 3.71 ppm, m, 4H), respectively. The signal at δ 4.99 ppm was the characteristic of the hydroxyl proton (δ_H = 4.99 ppm, t, 2H) (Imran et al. 2013).

In the ^{13}C-NMR spectrum, the signal at 59.00 ppm represented the carbon in the methylene group adjacent to the hydroxyl group, and the signal at 67.06 ppm indicated the presence of carbon in the methylene group next by the –COO– group. Signals at 129.54 and 133.76 ppm were given aromatic carbon associated with the hydrogen and –COO– groups, respectively. The signal at 165.19 ppm indicates carbon in the –COO– group. The NMR spectrum of the monomers produced in this study is identical to that reported in the literature (Lima et al. 2017) and verifies the high purity level of the monomers produced.

The main product obtained in PET glycolysis on ethylene glycol catalyzed by calcined ostrich eggshells at 1000 °C was confirmed by GC–MS (Fig. 14). The product showed a high purity, since no extra peak was found. It is clear from ESI–MS in Fig. 15 that the peak up to *m/z* 277 was obtained. This peak was related to the main product ionized by Na^+ (in electrospray ionization, the fraction can be ionized by H^+, Na^+, or K^+). Thus, the molecular weight of the main product was 254 g mol^{-1}, the amount equal to the molecular weight of the BHET.

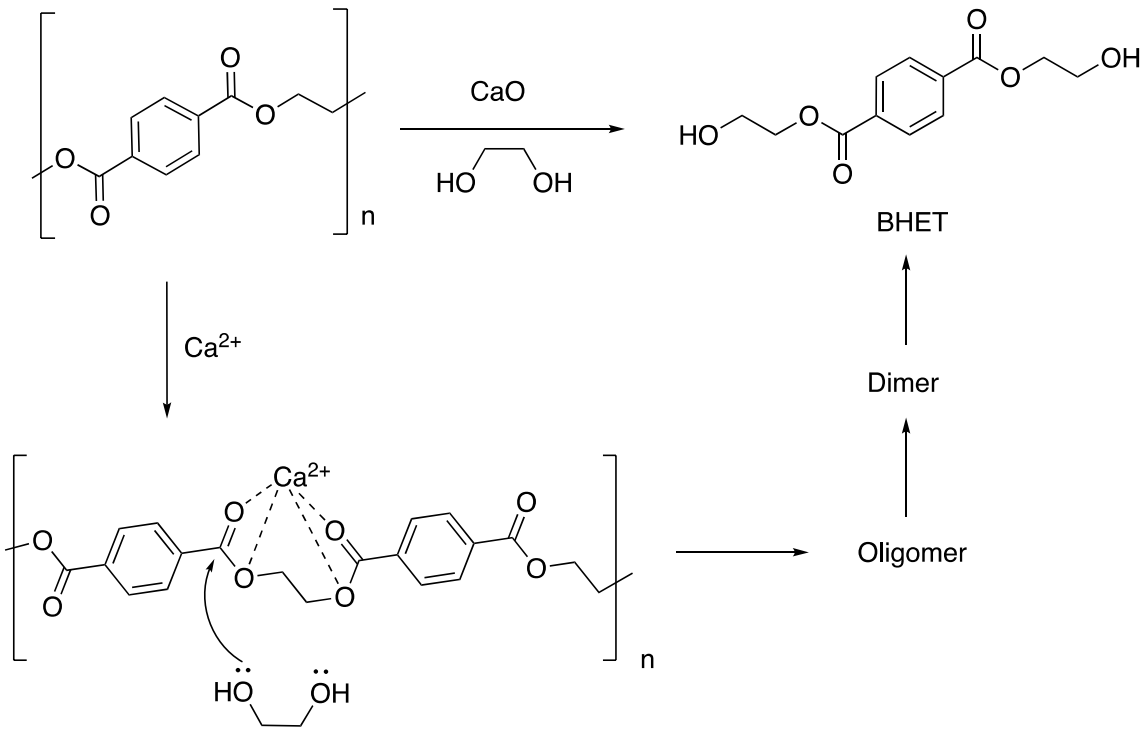

Scheme 1 A proposed mechanism of the glycolysis of PET catalyzed by CaO

The FTIR (KBr) spectrum of the purified monomer clearly is shown in Fig. 16 and Table 3. Furthermore, the peaks in the absorption band of about 3400 cm^{-1} belonging to the hydroxyl group did not appear in PET (Zhao et al. 2018), followed by the appearance of peaks in the spectrum of product indicating a successful breakdown of PET by ethylene glycol in the presence of CaO as a catalyst. The melted PET material which was further depolymerized into chemicals with less molecular weight including richer hydroxyl was confirmed by a sharper absorption peak between 3000 and 3500 cm^{-1}.

Based on our data, a proposed mechanism of the glycolysis of PET catalyzed by CaO is shown in Scheme 1. First, the complexation between Ca^{2+} and PET was formed to enhance the electrophilicity of the carbon of C=O and then the incoming of ethylene glycol to attack at the carbon of C=O to yield a hydroxyethyl terminal. The repeating reactions yielded oligomers, dimers, and BHET as products. According to the investigation of the effect of ratio of catalyst–PET on the yield of BHET (Fig. 11), the increase of the catalyst loading increased the basicity of the reaction resulting in the higher concentration of hydroxide ions. This led to the hydrolysis of PET and the lower yield of BHET because terephthalic acid and ethylene glycol were produced as by-products.

Conclusions

This work presented a promising catalyst, which was the by-product of eggshells and seafood shells on the glycolysis of poly(ethylene terephthalate) waste with bis(2-hydroxyethyl terephthalate) as the major products. The effects of catalyst, weight ratio of catalyst, weight ratio of solvent, depolymerization time were investigated. The results showed that the best condition in this work was 1 wt% of ostrich eggshells calcined at 1000 °C to run PET glycolysis at 192 °C for 2 h with a weight ratio of catalyst–PET at 1:10 and the ratio of weight of PET–ethylene glycol (EG) at 1:15, yielding 76.41% of BHET. This result was interestingly higher than the control experiment using commercial zinc acetate which produced 75.47% of BHET product. These findings suggested that CaO from by-products of the ostrich eggshells was promising for the depolymerization of water drinking bottles due to its low cost, environmentally friendly and high percent yield of the desired product.

Acknowledgements The authors gratefully acknowledge for financial support provided by Science and Technology Postgraduate Education and Research Development Office (PERDO) and Center of Excellence for Innovation in Chemistry (PERCH-CIC), the Directorate General of Resources for Science Technology and Higher Education, Ministry of Research, Technology and Higher Education (RISTEKDIKTI), the Republic of Indonesia, the Thailand Research Fund (RSA6080010) and the Royal Golden Jubilee Scholarship to PC [PHD/01242556]. On behalf of all authors, the corresponding author states that there is no conflict of interest.

References

Al-Sabagh AM, Yehia FZ, Eissa AMF, Moustafa ME, Eshaq G, Rabie AM, ElMetwally AE (2014) Cu- and Zn-acetate-containing ionic liquids as catalysts for the glycolysis of poly(ethylene terephthalate). Polym Degrad Stab 110:364–377. https://doi.org/10.1016/j.polymdegradstab.2014.10.005

Al-Sabagh AM, Yehia FZ, Harding DRK, Eshaq G, ElMetwally AE (2016) Fe_3O_4-boosted MWCNT as an efficient sustainable catalyst for PET glycolysis. Green Chem 18(14):3997–4003. https://doi.org/10.1039/C6GC00534A

Bartolome L, Imran M, Lee KG, Sangalang A, Ahn JK, Kim DH (2014) Superparamagnetic γ-Fe_2O_3 nanoparticles as an easily recoverable catalyst for the chemical recycling of PET. Green Chem 16(1):279–286. https://doi.org/10.1039/C3GC41834K

Buasri A, Chaiyut N, Loryuenyong V, Worawanitchaphong P, Trongyong S (2013) Calcium oxide derived from waste shells of mussel, cockle, and scallop as the heterogeneous catalyst for biodiesel production. Sci World J. https://doi.org/10.1155/2013/460923

Choudhary S, Surekha P, Kumar D, Rajagopal C, Roy P (2013) Microwave assisted glycolysis of poly(ethylene terepthalate) for preparation of polyester polyols. J Appl Polym Sci. https://doi.org/10.1002/app.38970

Duque-Ingunza I, López-Fonseca R, de Rivas B, Gutiérrez-Ortiz I (2013) Synthesis of unsaturated polyester resin from glycolysed postconsumer PET wastes. J Mater Cycles Waste Manage. https://doi.org/10.1007/s10163-013-0117-x

George N, Kurian T (2014) Recent developments in the chemical recycling of postconsumer poly(ethylene terephthalate) waste. Ind Eng Chem Res 53(37):14185–14198. https://doi.org/10.1021/ie501995m

Ghaemy M, Mossaddegh K (2005) Depolymerisation of poly(ethylene terephthalate) fibre wastes using ethylene glycol. Polym Degrad Stab 90(3):570–576. https://doi.org/10.1016/j.polymdegradstab.2005.03.011

Imran M, Lee K, Imtiaz Q, Kim BK, Han M, Cho BG, Kim DH (2011) Metal-oxide-doped silica nanoparticles for the catalytic glycolysis of polyethylene terephthalate. J Nanosci Nanotechnol 11(1):824–828. https://doi.org/10.1166/jnn.2011.3201

Imran M, Kim DH, Al-Masry WA, Mahmood A, Hassan A, Haider S, Ramay SM (2013) Manganese-, cobalt-, and zinc-based mixed-oxide spinels as novel catalysts for the chemical recycling of poly(ethylene terephthalate) via glycolysis. Polym Degrad Stab 98(4):904–915. https://doi.org/10.1016/j.polymdegradstab.2013.01.007

Jehanno C, Flores I, Dove AP, Müller AJ, Ruipérez F, Sardon H (2018) Organocatalysed depolymerisation of PET in a fully sustainable cycle using thermally stable protic ionic salt. Green Chem 20(6):1205–1212. https://doi.org/10.1039/C7GC03396F

Khoonkari M, Haghighi AH, Sefidbakht Y, Shekoohi K, Ghaderian A (2015) Chemical recycling of PET wastes with different catalysts. Int J Polym Sci. https://doi.org/10.1155/2015/124524

Lima GR, Monteiro WF, Ligabue R, Santana RMC (2017) Titanate nanotubes as new nanostrutured catalyst for depolymerization of PET by glycolysis reaction. Mat Res 20:588–595

López-Fonseca R, Duque-Ingunza I, de Rivas B, Arnaiz S, Gutiérrez-Ortiz JI (2010) Chemical recycling of post-consumer PET wastes

by glycolysis in the presence of metal salts. Polym Degrad Stab 95(6):1022–1028. https://doi.org/10.1016/j.polymdegradstab.2010.03.007

López-Fonseca R, Duque-Ingunza I, de Rivas B, Flores-Giraldo L, Gutiérrez-Ortiz JI (2011) Kinetics of catalytic glycolysis of PET wastes with sodium carbonate. Chem Eng J 168(1):312–320. https://doi.org/10.1016/j.cej.2011.01.031

Mohamad SFS, Mohamad S, Jemaat Z (2016) Study of calcination condition on decomposition of calcium carbonate in waste cockle shell to calcium oxide using thermal gravimetric analysis. ARPN JEAS 11:9917–9921

Mohamed M, Yousuf S, Maitra S (2012) Decomposition study of calcium carbonate in cockle shell. JESTEC 7:1–10

Nica S, Hanganu A, Tanase A, Duldner M, Iancu S, Draghici C, Bartha E (2015) Glycolytic depolymerization of polyethylene terephtalate (PET) wastes. Rev Chim Bucharest 66(8):1105–1111

Nikje MMA, Nazari F (2007) Microwave-assisted depolymerization of poly(ethylene terephthalate) [PET] at atmospheric pressure. Adv Polym Techn 25(4):242–246. https://doi.org/10.1002/adv.20080

Park G, Bartolome L, Lee KG, Lee SJ, Kim DH, Park TJ (2012) One-step sonochemical synthesis of a graphene oxide–manganese oxide nanocomposite for catalytic glycolysis of poly(ethylene terephthalate). Nanoscale 4(13):3879–3885. https://doi.org/10.1039/C2NR30168G

Pingale ND, Shukla SR (2008) Microwave assisted ecofriendly recycling of poly (ethylene terephthalate) bottle waste. Eur Polym J 44(12):4151–4156. https://doi.org/10.1016/j.eurpolymj.2008.09.019

Pingale ND, Palekar VS, Shukla SR (2010) Glycolysis of postconsumer polyethylene terephthalate waste. J Appl Polym Sci 115(1):249–254. https://doi.org/10.1002/app.31092

Shukla SR, Harad AM (2005) Glycolysis of polyethylene terephthalate waste fibers. J Appl Polym Sci 97(2):513–517. https://doi.org/10.1002/app.21769

Shukla SR, Kulkarni KS (2002) Depolymerization of poly(ethylene terephthalate) waste. J Appl Polym Sci 85(8):1765–1770. https://doi.org/10.1002/app.10714

Tan YH, Abdullah MO, Nolasco-Hipolito C, Taufiq-Yap YH (2015) Waste ostrich- and chicken–eggshells as heterogeneous base catalyst for biodiesel production from used cooking oil: catalyst characterization and biodiesel yield performance. Appl Energy 160:58–70. https://doi.org/10.1016/j.apenergy.2015.09.023

Troev K, Grancharov G, Tsevi R, Gitsov I (2003) A novel catalyst for the glycolysis of poly(ethylene terephthalate). J Appl Polym Sci 90:1148–1152. https://doi.org/10.1002/app.12711

Viriya-empikul N, Krasae P, Nualpaeng W, Yoosuk B, Faungnawakij K (2012) Biodiesel production over Ca-based solid catalysts derived from industrial wastes. Fuel 92(1):239–244. https://doi.org/10.1016/j.fuel.2011.07.013

Wang H, Liu Y, Li Z, Zhang X, Zhang S, Zhang Y (2009) Glycolysis of poly(ethylene terephthalate) catalyzed by ionic liquids. Eur Polym J 45(5):1535–1544. https://doi.org/10.1016/j.eurpolymj.2009.01.025

Webb KH, Arnott J, Crawford JR, Ivanova PE (2013) Plastic degradation and its environmental implications with special reference to poly(ethylene terephthalate). Polymers 5(1):1–18. https://doi.org/10.3390/polym5010001

Xi G, Lu M, Sun C (2005) Study on depolymerization of waste polyethylene terephthalate into monomer of bis(2-hydroxyethyl terephthalate). Polym Degrad Stab 87(1):117–120. https://doi.org/10.1016/j.polymdegradstab.2004.07.017

Zhao Y, Liu M, Zhao R, Liu F, Ge X, Yu S (2018) Heterogeneous CaO(SrO, BaO)/MCF as highly active and recyclable catalysts for the glycolysis of poly(ethylene terephthalate). Res Chem Intermed 44(12):7711–7729. https://doi.org/10.1007/s11164-018-3582-y